International Journal of Applied Engineering Research ISSN 0973-4562 Volume 13, Number 14 (2018) pp. 11402-110409

Controller Design for Snake Robots

Ruben D. Hernández[1], Oscar F. Avilés[2], Jonathan A. Bermudez[3], Claudia T. Martinez[4]

[1]*Professor, Department of Mechatronics Engineering, Piloto University of Colombia, Bogotá, Colombia.*

[2]*Professor, Department of Mechatronics Engineering, Piloto University of Colombia, Bogotá, Colombia.*

[3]*Assistant research, Department of Mechatronics Engineering, Piloto University of Colombia, Bogotá, Colombia.*

[4]*Assistant research, Department of Mechatronics Engineering, Piloto University of Colombia, Bogotá, Colombia.*

Abstract

Exploratory robots of the snake type are a class of mobile robots designed to move in places of difficult access like cracks and pipes, thanks to the movement of meander derived from the sinusoidal movement characteristic of this type of robot to lack of limbs that facilitate its displacement. Deepening the study of the snake robots it is found that they lack a control system, causing them to be usually controlled by means of pre-programmed movement sequences or are also controlled at a distance, i.e. their movements are tele operated. Due to this, this work was carried out with the purpose of proposing a control system based on the kinematic model, studying different controllers such as proportional controller, diffuse controller and proportional-diffuse controller; Seeking to correct the error of the locomotion presented by the robot in a path that considers various factors such as meandering angle, length of modules, number of modules, among others.

Keywords: Snake angle, fuzzy controller, proportional controller, proportional diffuse controller, modules, sine motion, meander motion, path tracking.

INTRODUCTION

The snake robot is a type of robot explorer designed to move in places of difficult access due to the little space required for its mobility, thanks to that quality is normally used in the industry for the exploration of pipes and cracks. Apex robots are robot bio-inspired in snake animals such as snakes and worms, emphasizing its structure and characteristic sinusoidal movement that allows a movement in different environments without much space [1-6].

The structure that makes up the body of the robot is made up of multiple modules which allow the sinusoidal movement to be generated, since it is the form used to move because it has no limbs that allow it to have another type of movement. As presented by Juan González Gómez [7] in his work "Main lines of research in snake type robots" in which he presents different lines of research for the snake robots explored by the Carnegie Mellon University in which he deepens in the line of search And rescue emphasizing the family of USAR robots, which implement cameras on the front and sensors that allows them to detect people amid debris. Another possible application of anode robots is the implementation in three-dimensional inspection, an example of that is the inspection of bridges where the welding points are checked, checking the good condition at the critical points of the structure reflecting the need of a control system with adequate trajectory, allowing to mobilize the system of appropriate form through the obstacles, the debris and in the structure of the bridges [8-9].

Another robot that was studied for use in the exploration of pipes is presented in the work "Design of a Modular Snake Robot" by Wright C.et.al. [10], where they present a robot serpent (Snake robot) of the climber type Thanks to the implementation of servomotors with the capacity to support the full weight of the sixteen (16) modules that make up the main structure of the robot. The presented serpent robot has the ability to mobilize both on the outside of the pipes by winding through the outer layer and internally using the meander movement according to the allowed angle of movement between the dimensions of the robot as the internal area Of the pipe.

The desired trajectory for the movement of the robot climber must consider both the inertia generated by its own structure and the desired trajectory, making the control system allow to follow the desired trajectory, highlighting the ineffectiveness of a sequence of movement developed around the change of the angle of the servomotors, thus generating the need to correct the path with respect to the variation of the meandering angle [11-13].

The structure composed of modules allows the robot components to be properly distributed, providing a correct operation in the electronic, mechanical and control systems for the proper tracking of the desired path based on the winding movement derived from the sinusoidal movement.

TRAJECTORY

The trajectory forms an important part in the analysis of exploratory robots of the snake type because it comprises both the physical limitations and the movement characteristics used for their displacement. The studied path is based on the sinuosity movement comprised in two dimensions (2D), but

being a robot of the type explorer the required movement is in three dimensions (3D); By understanding the interaction between the modules since the rotation of ninety degrees (90 degrees) between the modules allows the displacement in the plane as it is exposed in the work of Juan González Gómez [14] or in the argument exposed in the work of Andrés San Millán Rodríguez [15] in which it also exposes the transmission of sinusoidal waves with which they allow the generation of serpentenoid curves.

In order to perform the kinematic analysis of the robot must take into account the parameters described below:

- Angle of winding (α): It is the angle generated between the robot segments and a reference axis in the plane where the sine wave is reflected.
- Offset Angle (φ): Understands the offset angle between the sine wave and the reference point.
- Number of modules (M): The modules are the main structure that makes up the body of the robot, the minimum number of modules necessary for the configuration of the robot structure is and the maximum will be limited according to the task assigned by the user when varying the number of cables, batteries, sensors, among others.
- Length of the module (L): The length is given by the measurement of the module when it is at rest, i.e the angle is 0 °. Because the segments are the same, each will consist of 2 modules.
- Length of the robot (l): When being built by equal modules the length of the robot will be found through the product between the length of the modules (L) with the number of these (M) so the equation is obtained $l = M \times L$.
- Distance along the curve (s): It is the distance between 0 and along the curve.
- Ripple Number (k): The number of ripples is the number of repetitions of the sine wave based on the length of the robot.
- Period (T): It is the time taken to carry out an induction. Taking into account the length parameters of the robot (l) and number of undulations (k)mentioned above, the equation can be generated $T = \frac{1}{k}$.
- Number of articulation (i): It comprises the number of the joint, of 1 up M

The above parameters can be visualized in Figure 1, in which the range and the measurement of the parameters are explained for their better understanding

The sinusoidal function is given by (1).

$$F(x) = A\sin(bx + c) \qquad (1)$$

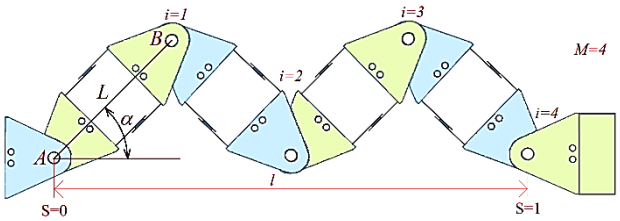

Figure 1. Display of parameters.

Replacing with the parameters and considering that it is based on the position space «s» as described by Hadi Kalani, Alireza Akbarzadeh, Hosseinel Bahrami [16] gives as a result (2).

$$K_{(s,\varphi)} = -\frac{2\Pi k}{l}\alpha\sin\left(\phi + \frac{2\Pi k}{l}s\right) \qquad (2)$$

To find the functions that correctly represent the meandering wave it is necessary to find the tangent form to the curve in (2).

$$\alpha_s = \alpha\cos\left(\phi + \frac{2\Pi k}{l}s\right) \qquad (3)$$

In order to find the coordinates in the plane it is necessary to integrate between and in (3) based on the cosine for the coordinates in and the sine in the coordinate in (4) and (5).

$$X_{(s,\varphi)} = \int \cos\left(\alpha\cos\left(\phi + \frac{-2\Pi k}{l}s\right)\right)ds \qquad (4)$$

$$Y_{(s,\varphi)} = \int \sin\left(\alpha\cos\left(\phi + \frac{-2\Pi k}{l}s\right)\right)ds \qquad (5)$$

One of the results of the equations previously found can be seen in Figure 2, where three red, green and blue sinusoidal waves corresponding to ninety degrees (90^o), sixty degrees (60^0) and forty five degrees (45^0) respectively.

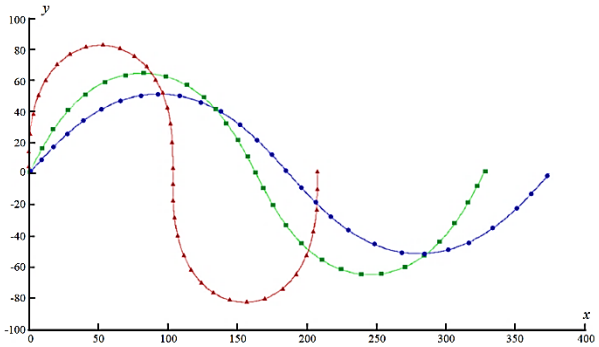

Figure 2. Winding angle variation.

The minimum winding angle is given by (6) obtained from [7], due to the change in the design of the robot used as the object of study and the maximum winding angle is given by (7) which can not exceed the angle 121^o of. In any case, if the maximum

angle is exceeded, it will cause a collapse between the points of the curve, so this restriction must be taken into account.

$$\alpha_{min} \approx \frac{120}{l}\left(\sqrt{\left(\frac{l}{L}\right)^2 + 18 - \frac{l}{L}}\right) \quad (6)$$

$$\alpha_{max} \approx \frac{A}{2\sin\left(\frac{\Pi k}{M}\right)} \leq 121 \quad (7)$$

The maximum angle that the snake robots can adopt is one hundred and twenty-one degrees (121^o)shown in Figure 3, showing a very pronounced curvature, thanks to which it was necessary to employ two undulations $(k = 2)$ for a better understanding of their shape.

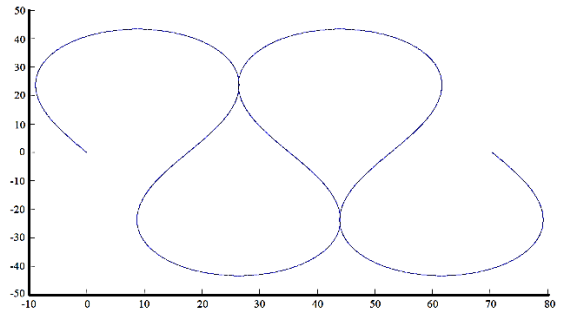

Figure 3. Winding wave with curvature of 121^o

Control Design

The designs of the controllers presented were developed around the kinematic model presented in the work "Kinematic Analysis of a Robot Type Apode" by Jonathan A. Bermudez M., Claudia T. Martinez S., Rubén D. Hernández B., Oscar Avilés S., João M. Rosario. [17-18] Presented for "V International Congress of Mechatronics Engineering and Automation - CIIMA Bucaramanga" in 2016.

Proportional Controller

The proportional controller is composed of two gains (K_1, K_2) which amplify the resulting error between the difference between the desired position and the current position of the robot as shown in the diagram of Figure 4, in which the position correction is exposed through the System feedback.

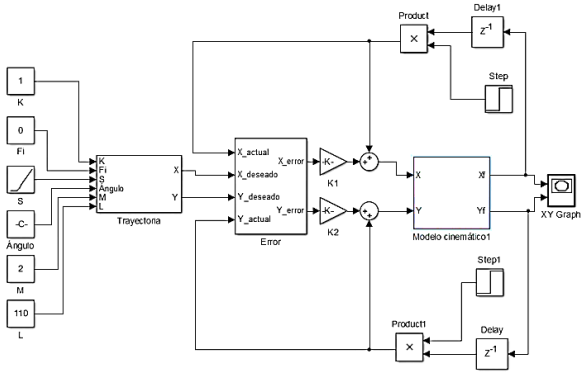

Figure 4. Proportional Controller.

To find the appropriate value of the gains K_1 and K_2 the table I was made, where the system error is evaluated considering the error in X denoted as E_x, the error Y in denoted as E_y and the total error that is given by the Euclidean distance denoted as E [19-20]. To obtain the Euclidean distance is used in (8) where it considers the error in both the axis and the axis y.

$$E = \sqrt{Ex^2 + Ey^2} \quad (8)$$

Table I. Variation of constants in proportional controller

K1	K2	Ex (%)	EY (%)	E (%)
2	2	2,1296	4,8603	5,3063
2	1,5	2,0201	7,2309	7,5077
2	1,1	1,9672	9,6659	9,8640
2	0,8	2,0247	12,9731	13,1301
2	0,2	1,5241	34,9816	35,0147
1,5	2	2,0996	7,0325	7,3392
1,5	1,5	2,2148	7,9471	8,2499
1,5	1,1	2,2303	9,7339	9,9861
1,5	0,8	2,2146	12,2307	12,4295
1,5	0,2	2,0308	34,9041	34,9631
1,1	2	2,8873	6,9005	7,4802
1,1	1,5	3,0248	7,8464	8,4092
1,1	1,1	3,0407	9,6376	10,1058
1,1	0,8	3,0174	12,1340	12,5035
1,1	0,2	2,7669	34,7926	34,9024
0,8	2	4,0140	6,7073	7,8166
0,8	1,5	4,1671	7,7046	8,7593
0,8	1,1	4,1785	9,5036	10,3820
0,8	0,8	4,1442	11,9999	12,6953
0,8	0,2	3,8002	34,6379	34,8457
0,2	2	16,7566	5,0680	17,5062
0,2	1,5	16,6940	6,3719	17,8722
0,2	1,1	16,5485	8,2318	18,4828
0,2	0,8	16,3446	10,7082	19,5399
0,2	0,2	15,0441	33,0640	36,3256

The variation of the gains used for the proportional controller demonstrates that from the variation the error can be reduced, as seen in Figure 5, where the values of $K_1 = 0.8$ and $K_2 = 2$ are shown, showing a suitable behavior to the desired controller, which can vary with the Selection of the incorrect variables as shown in Figure 6 where the values of K_1 and K_2 are equal to 2 increasing the margin of error.

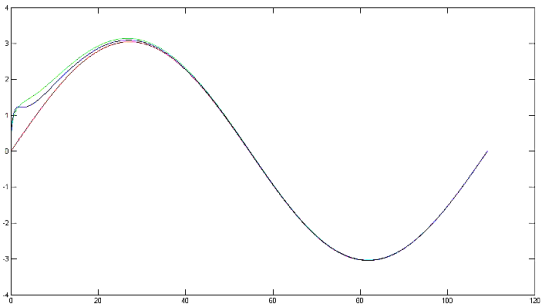

Figure 5. Proportional controller desired results

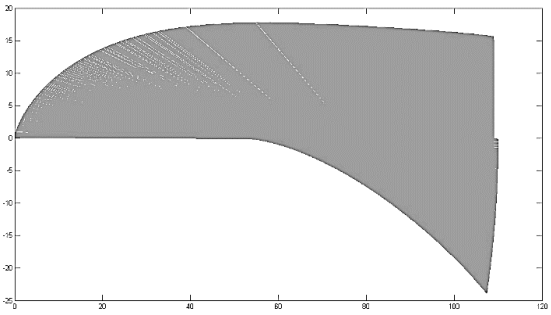

Figure 6. Proportional controller desired results

Fuzzy Controller

The kinematic model studied exposes a nonlinear system, so that a controller suitable for implementation in the system is the diffuse controller based on fuzzy logic. Applying the fuzzy logic around the implemented kinematic model is presented the controller of Figure 7 by block diagram.

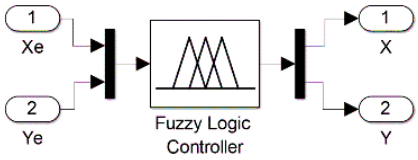

Figure 7. Fuzzy Controller

The error is used as a basis for the design of the controller as the reference for the desired behavior, due to which it was necessary to use two error inputs representing the deviation of the resulting trajectory in axis X and in the axis Y, to plan the trajectory of Appropriate form are established some membership functions together with their rules.

Relevance Functions

In order to establish the behavior of the controller, 9 membership functions are established that provide a great accuracy in trajectory tracking and signal smoothing around the desired behavior, because the membership functions are of the Gaussian type as shown in Figure 8 and Figure 9, where the input variables X_e and Y_e respectively corresponding to the error inputs in X and Y are exposed.

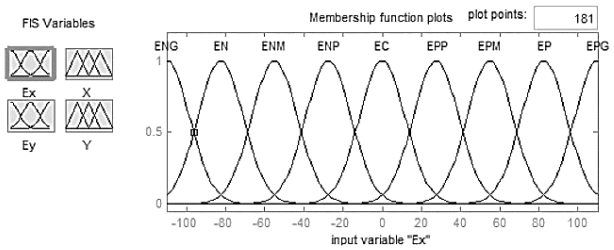

Figure 8. X coordínate error input variables

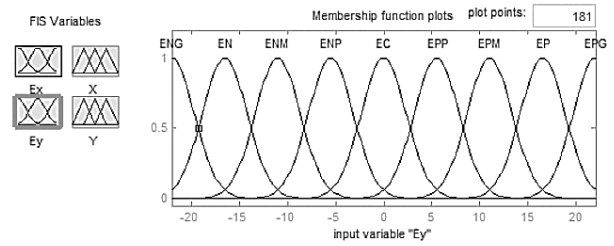

Figure 9. Y coordínate error input variables

The parameters of the output signal from the controller to the system implement membership functions similar to the input, due to the function of correction of the desired error for the system, allowing to establish rules in a simple and efficient way where the outputs seen in Figure 10 corresponding to the output X in and Figure 11 corresponding to the output in Y.

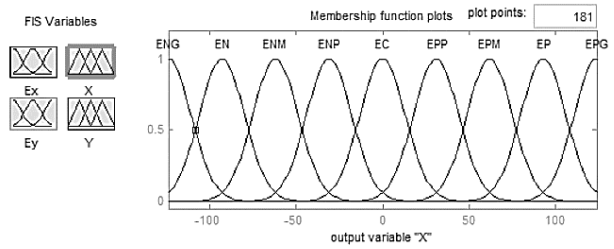

Figure 10. X Coordinate controller output variables

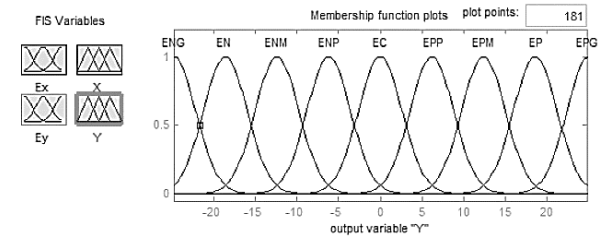

Figure 11. Y Coordinate controller output variables

For reasons of space, abbreviations were used to name the different membership functions, where: ENG corresponds to the "Large negative error", EN is the "Negative error", ENM corresponds to the "Mean negative error", ENP is the "Small negative error", EC corresponding to "Zero error", EPP is called "Small positive error"', EPM corresponds to "Mean positive error", EP belonging to "Positive error" and lastly, EPG corresponding to "Large positive error".

Table II. Fuzzy rules implemented

Membership function	ENG in Xe	EN in Xe	ENM In Xe	ENP In Xe	EC In Xe	EPP In Xe	EPM In Xe	EP In Xe	EPG In XE
ENG in Ye	X=EPG Y=EPG	X=EP Y=EPG	X=EPM Y=EPG	X=EPP Y=EPG	X=EC Y=EPG	X=ENP Y=EPG	X=ENM Y=EPG	X=ENG Y=EPG	X=ENG Y=EPG
EN in Ye	X=EPG Y=EP	X=EP Y=EP	X=EPM Y=EP	X=EPP Y=EP	X=EC Y=EP	X=ENP Y=EP	X=ENM Y=EP	X=ENG Y=EP	X=ENG Y=EP
ENM In Ye	X=EPG Y=EPM	X=EP Y=EPM	X=EPM Y=EPM	X=EPP Y=EPM	X=EC Y=EPM	X=ENP Y=EPM	X=ENM Y=EPM	X=ENG Y=EPM	X=ENG Y=EPM
ENP In Ye	X=EPG Y=EPP	X=EP Y=EPP	X=EPM Y=EPP	X=EPP Y=EPP	X=EC Y=EPP	X=ENP Y=EPP	X=ENM Y=EPP	X=ENG Y=EPP	X=ENG Y=EPP
EC In Ye	X=EPG Y=EC	X=EP Y=EC	X=EPM Y=EC	X=EPP Y=EC	X=EC Y=EC	X=ENP Y=EC	X=ENM Y=EC	X=ENG Y=EC	X=ENG Y=EC
EPP In Ye	X=EPG Y=ENP	X=EP Y=ENP	X=EPM Y=ENP	X=EPP Y=ENP	X=EC Y=ENP	X=ENP Y=ENP	X=ENM Y=ENP	X=ENG Y=ENP	X=ENG Y=ENP
EPM In Ye	X=EPG Y=ENM	X=EP Y=ENM	X=EPM Y=ENM	X=EPP Y=ENM	X=EC Y=ENM	X=ENP Y=ENM	X=ENM Y=ENM	X=ENG Y=ENM	X=ENG Y=ENM
EP In Ye	X=EPG Y=EN	X=EP Y=EN	X=EPM Y=EN	X=EPP Y=EN	X=EC Y=EN	X=ENP Y=EN	X=ENM Y=EN	X=ENG Y=EN	X=ENG Y=EN
EPG In YE	X=EPG Y=ENG	X=EP Y=ENG	X=EPM Y=ENG	X=EPP Y=ENG	X=EC Y=ENG	X=ENP Y=ENG	X=ENM Y=ENG	X=ENG Y=ENG	X=ENG Y=ENG

Fuzzy rules

The diffuse rules used to control the implemented system are based on the concept of error correction, causing the output of the variables used to be opposed to the input variables, because the controller is based on the position error in the coordinates (X, Y) Allowing to correct the position that follows the trajectory, thus obtaining Table II.

In the context of diffuse rules, Figure 12 shows the response of the membership functions resulting from the application of the fuzzy rules observed above, showing the magnitude of the obtained values.

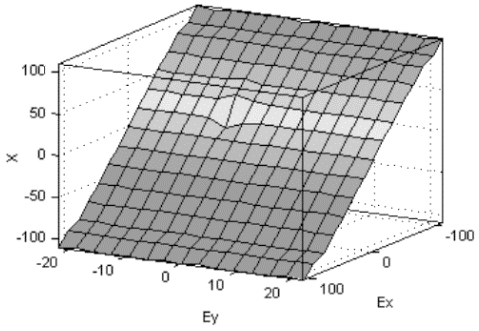

Figure 12. Fuzzy controller surface

Having raised the rules of the controller, the fuzzy controller is continued using the block diagram shown in Figure 13 where the delay in the position feedback is shown to find the error in the coordinates surrounding the current position, position Desired by the path, causing the initial coordinates given by the "Step" pulse and the position where it starts at zero using the delay time as reference. Also the current positioning is observed being retro-feeding to the input of the system being added with the controller, providing the change of position around the error.

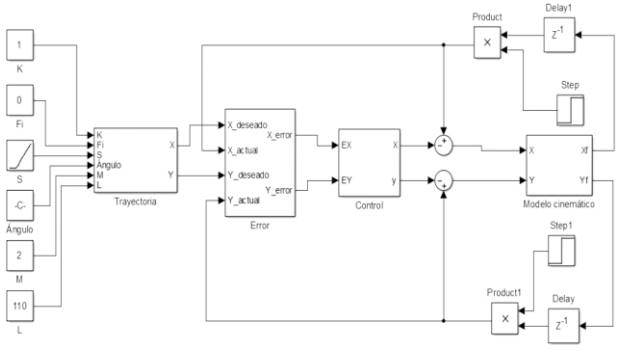

Figure 13. Fuzzy controller diagram

Using the block diagram of the fuzzy control shown in Figure 13, there are shown Figures 14, 15 and 16, showing the blue output of the system using the controller and red the input path to the system where it is reflected A minimal correction of the path error, due to this it is necessary to complement the controller to improve the response. In addition, there is a lack of control against angles greater than 10^o as seen in Figure 15 belonging to the angle of 90^o and Figure 16 corresponding to the angle of twisting of 121^o that present greater error and surpass the angle of meandering greater than the recommended one of 30^o.

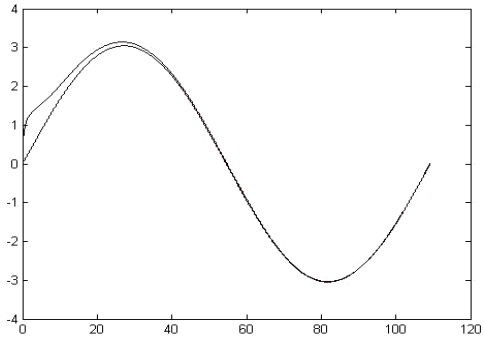

Figure 14. Fuzzy controller result with angle of 10^o

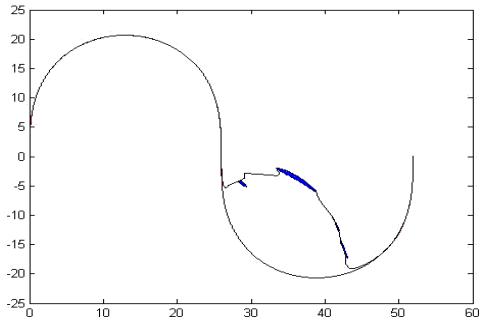

Figure 15. Fuzzy controller result with angle of 90^o

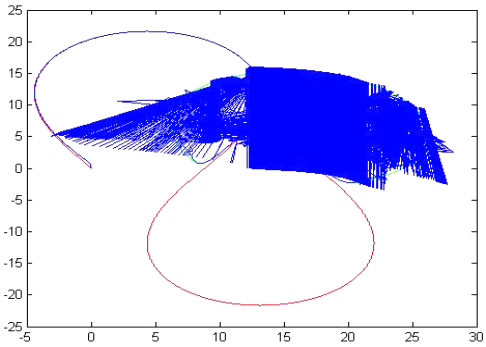

Figure 16. Fuzzy controller result with angle of e 121^o

Figure 14 shows the increase in the Error with respect to Figures 15 and 16, caused by the increase of the meandering angle caused by the limitations presented by the modules. The uncontrolled presented by the system in the course of the trajectory is attributed not only to the limitations presented by the module as mentioned above, due to the necessity presented to control each module against the displacement, reason why when increasing the number of modules They must increase the number of controllers.

Fuzz- Proportional Controller

The proportional-diffuse controller is proposed as the union of the controllers already seen proportional and diffuse, so the controller is shown in Figure 17, where the controller inputs are amplified by two gain variables $(K1, K2)$, which amplify or reduce the error Obtaining a faster or slow response according to the necessity presented.

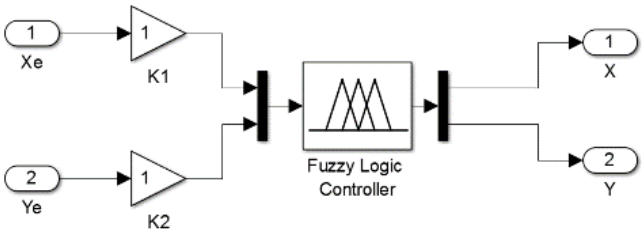

Figure 17. Fuzzy Proportional controller

In order to find the most appropriate variables for the proposed system, Table III is performed, where gains are varied and as was done previously, thanks to the change in the response caused by the diffuse controller seen above.

Table III

Variation of constants of fuzzy proportional controller

K1	K2	Ex (%)	EY (%)	E (%)
2	2	4,679	5,8088	7,4589
2	1,5	2,2918	6,7859	7,1642
2	1,1	34,8878	151,4378	155,4045
2	0,8	168,8941	207,7802	267,7645
2	0,2	1,1256	15,151	15,1927
1,5	2	0,8381	6,2057	6,2620
1,5	1,5	1,5036	2,8558	3,2274
1,5	1,1	1,5117	3,8104	4,0993
1,5	0,8	1,4621	4,9858	5,1957
1,5	0,2	1,4274	17,9622	18,0188
1,1	2	0,6750	8,842	8,8677
1,1	1,5	1,976	3,1734	3,7383
1,1	1,1	2,013	4,3607	4,8029
1,1	0,8	1,9613	5,7489	6,0742
1,1	0,2	1,91	20,7673	20,8549
0,8	2	1,3573	5,9846	6,1365
0,8	1,5	2,6249	3,0639	4,0345
0,8	1,1	2,8362	4,411	5,2441
0,8	0,8	2,7457	5,3915	6,0503
0,8	0,2	2,6701	19,6124	19,7933
0,2	2	10,5289	2,0387	10,7244
0,2	1,5	10,954	2,8819	11,3267
0,2	1,1	10,941	3,9562	11,6343
0,2	0,8	11,7051	5,8388	13,0805
0,2	0,2	13,0816	26,4647	29,5213

Table III shows the system error in relation to the profit variation. By varying the gains, a quick and precise response is obtained, which reduces the margin of error by using the appropriate values as they are K_1 and K_2 equal to 1.5 with a margin of error of 3.2274%, a considerable decrease as seen in Figure 18.

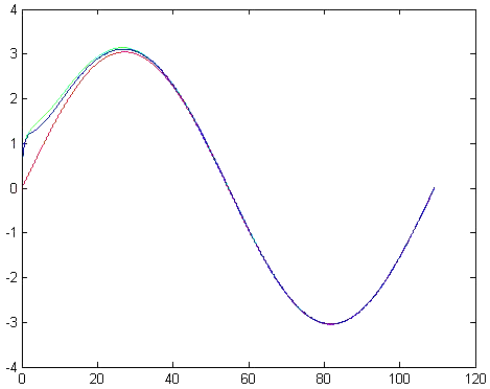

Figure 18. Response fuzzy proportional controller

RESULTS

Observing the results of the different controllers studied above, different behaviors with respect to the variation of parameters are obtained obtaining the gains and, therefore, different error margins are also found which present both an increase of the error and a decrease according to the variation of these. Analyzing this variation, the parameters with which the system presented the lowest margin of error and with which the table IV is performed, where the errors in the axis and the axis along with the resulting average error are shown. In addition, the decrease of the error in front of the controller change is emphasized, so that the proportional-diffuse controller presents an optimal decrease of the margin of error.

Table IV

Characteristics of the controllers

Controller	E_X(%)	E_Y(%)	Total Error
Proportional	4.0140	6.7073	7.8166
Fuzzy	2.5622	6.2257	6.7323
Fuzzy-proportional	1.5036	2.8558	3.2274

The controllers studied have different behaviors based on the changes of parameters presented as is the variation of the angle of winding. Therefore, Table V was presented which presents the advantages and disadvantages of the controllers according to the change of parameters.

CONCLUSIONS

In this work, we have analyzed the different factors involved in the locomotion of snake type robots, in order to propose a suitable trajectory that reflects an appropriate behavior for the system, allowing the proposal of different control systems.

As mentioned previously, different factors to be considered for the locomotion of this type of robot were analyzed in order to propose a suitable trajectory for the robot. One of these factors to consider is the angle of meandering to be the angle in which initiates its sinusoidal movement characteristic of this type of robot.

Table V

Advantages and disadvantages

Controller	Advantages	Disadvantages
Proportional	It presents higher processing speed and adequate reduction of the error of grafic form	Improper meandering tends to increase the margin of error
Fuzzy	Adequate and constant behavior at suitable winding angles for the system	It tends to be out of control in the face of inadequate winding angles due to the number of modules that make up the robot structure
Fuzzy-proportional	The result of its application reflects a suitable behavior both in the angle of winding, as in the abrupt variations that could suffer.	Although it presents better behavior, it tends to be uncontrollable in the face of inadequate snaking angles, but with a smaller margin of error

However, it is necessary to consider the limitations of that factor because its limitation is given by the number of modules and length of each one of mathematical form independent of the mechanical design and of the parameters given by the type of motor selected.

Thanks to the trajectory proposed and the kinematic model [4], it is possible to study different types of controllers with different qualities, such as the proportional control system that allows a faster response suitable for the robots of the explorer class when having the need to react of fast way against the changes of movement unlike the diffuse control system studied that presents a lower speed but greater control and precision against the inadequate changes in the angle of serpent mentioned above, reason why it is applicable in zones of controlled exploration as the pipes that require more precision instead of velocity, and finally, the proportional controller was the one that presented the least margin of error when combining the qualities seen in both the proportional controller and the diffuse controller, facilitating the control for both the motion analysis and Exploration in controlled areas.

ACKNOWLEDGEMENT

This work was supported by the INNOVATIC in the Department of Mechatronics Engineering of Piloto de Colombia

REFERENCES

[1] R. YAMASHINA, M. KURODA and T. YABUTA, "Caterpillar Robot Locomotion Based on Reinforcement Learning Using Subjective Reward", TRANSACTIONS OF THE JAPAN SOCIETY OF MECHANICAL ENGINEERS Series C, vol. 79, no. 798, pp. 366-370, 2013.

[2] H. Lin, G. Leisk and B. Trimmer, "GoQBot: a caterpillar-inspired soft-bodied rolling robot", Bioinspiration & Biomimetics, vol. 6, no. 2, p. 026007, 2011.

[3] W. Cui, W. Wang, L. Zhao and H. Zhang, "Flexible Structural Design for Side-Sliding Force Reduction for a Caterpillar Climbing Robot", International Journal of Advanced Robotic Systems, vol. 9, no. 5, p. 198, 2012.

[4] K. Wang, W. Wang and H. Zhang, "Analysis of Gait and Mechanical Property of Wall-climbing Caterpillar Robot", Journal of Computers, vol. 7, no. 3, 2012.

[5] D. Kim, H. Hong, H. Kim and J. Kim, "Optimal design and kinetic analysis of a stair-climbing mobile robot with rocker-bogie mechanism", Mechanism and Machine Theory, vol. 50, pp. 90-108, 2012.

[6] K. Wang, W. Wang and H. Zhang, "Development and Experiment of Wall-Climbing Caterpillar Robot", Advanced Materials Research, vol. 308-310, pp. 2031-2036, 2011

[7] Juan González Gómez. Principales líneas de investigación en robots tipo ápodos. 2002.

[8] W. Cui, W. Wang, L. Zhao and H. Zhang, "Flexible Structural Design for Side-Sliding Force Reduction for a Caterpillar Climbing Robot", International Journal of Advanced Robotic Systems, vol. 9, no. 5, p. 198, 2012.

[9] T. Umedachi, K. Ito and A. Ishiguro, "Soft-bodied amoeba-inspired robot that switches between qualitatively different behaviors with decentralized stiffness control", Adaptive Behavior, vol. 23, no. 2, pp. 97-108, 2015.

[10] Cornell Wright, Aaron Johnson, Aaron Peck, Zachary Mccord, Allison Naaktgeboren, Philip Gianfortoni, Manuel Gonzalez-rivero, Ross Hatton, and Howie Choset. Design of a modular snake robot.

[11] K. Cho, H. Kim, Y. Jin, F. Liu, H. Moon, J. Koo and H. Choi, "Inspection Robot for Hanger Cable of Suspension Bridge: Mechanism Design and Analysis", IEEE/ASME Transactions on Mechatronics, vol. 18, no. 6, pp. 1665-1674, 2013.

[12] G. Li, H. Zhang, J. Zhang and R. Bye, "Development of adaptive locomotion of a caterpillar-like robot based on a sensory feedback CPG model", Advanced Robotics, vol. 28, no. 6, pp. 389-401, 2014.

[13] H. Zeng, O. Wani, P. Wasylczyk and A. Priimagi, "Light-Driven, Caterpillar-Inspired Miniature Inching Robot", Macromolecular Rapid Communications, p. 1700224, 2017.

[14] Juan González Gómez. Robótica modular y locomoción: Aplicación a robots ápodos. Universidad Autónoma de Madrid, Thesis, 2008.

[15] Andrés San Millán Rodríguez. Diseño, construcción y control de una serpiente robótica. In Creatividad, descubrimiento y futuro: I Congreso Nacional de Investigación en Grado INVESGRADO 2011, Albacete, Junio de 2011, pages 1385–1399. Universidad de Castilla-La Mancha, 2011.

[16] Hadi Kalani, Alireza Akbarzadeh, and Hossein Bahrami. Application of statistical techniques in modeling and optimization of a snake robot. Robotica, 31(4):623–641, 07 2013. Copyright – Copyright©, Cambridge University Press 2012; Última actualización - 2013-05-24.

[17] Ricardo A. Castillo, Oscar F. Avilés, Oscar G. Rubiano, "Review of Connector Docking Systems for Modular Robotic Systems", International Review of Mechanical Engineering (IREME). Vol 10, No 2 (2016) ISSN: 1970-8734 https://doi.org/10.15866/ireme.v10i2.7492

[18] Rubén D. Hernández B y Oscar Avilés S. Jonathan A. Bermúdez M, Claudia T. Martínez S. Análisis cinemático de un robot ápodo. V Congreso Internacional de Ingeniería Mecatrónica y Automatización CIIMA, 2016.

[19] M. Rogóż, H. Zeng, C. Xuan, D. Wiersma and P. Wasylczyk, "Light-Driven Soft Robot Mimics Caterpillar Locomotion in Natural Scale", Advanced Optical Materials, vol. 4, no. 11, pp. 1689-1694, 2016.

[20] G. Li, H. Zhang, J. Zhang and R. Bye, "Development of adaptive locomotion of a caterpillar-like robot based on a sensory feedback CPG model", Advanced Robotics, vol. 28, no. 6, pp. 389-401, 2014.